

Evidence of potential change in nonsequential double ionization

Changchun Jia(贾昌春), Pu Zhang(张朴), Hua Wen(文华), and Zhangjin Chen(陈长进)
Citation: Chin. Phys. B, 2021, 30 (**2**): 023401. DOI: 10.1088/1674-1056/abc151
Journal homepage: http://cpb.iphy.ac.cn; http://iopscience.iop.org/cpb

What follows is a list of articles you may be interested in

Quantitative rescattering theory for nonsequential double ionization

Zhangjin Chen(陈长进), Fang Liu(刘芳), Hua Wen(文华)
Chin. Phys. B, 2019, 28 (**12**): 123401. DOI: 10.1088/1674-1056/ab54b3

Relativistic electron scattering from freely movable proton/μ^+ in the presence of strong laser field

Ningyue Wang(王宁月), Liguang Jiao(焦利光), Aihua Liu(刘爱华)
Chin. Phys. B, 2019, 28 (**9**): 093402. DOI: 10.1088/1674-1056/ab343e

Interference effect of photoionization of hydrogen atoms by ultra-short and ultra-fast high-frequency chirped pulses

Ningyue Wang(王宁月), Aihua Liu(刘爱华)
Chin. Phys. B, 2019, 28 (**8**): 083403. DOI: 10.1088/1674-1056/28/8/083403

Theoretical simulation of the photoassociation process for NaCs

Zhang Chang-Zhe, Zheng Bin, Wang Jun, Meng Qing-Tian
Chin. Phys. B, 2013, 22 (**2**): 023401. DOI: 10.1088/1674-1056/22/2/023401

High sensitive detection of high-order partial wave scattering in photoassociation of ultralcold atoms

Li Yu-Qing,Ma Jie,Wu Ji-Zhou,Zhang Yi-Chi,Zhao Yan-Ting,Wang Li-Rong,Xiao Lian-Tuan,Jia Suo-Tang
Chin. Phys. B, 2012, 21 (**4**): 043404. DOI: 10.1088/1674-1056/21/4/043404

Evidence of potential change in nonsequential double ionization*

Changchun Jia(贾昌春)[1,†], Pu Zhang(张朴)[2], Hua Wen(文华)[2], and Zhangjin Chen(陈长进)[2,‡]

[1] School of Physics and Material Science, Anhui University, Hefei 230039, China
[2] Department of Physics, College of Science, Shantou University, Shantou 515063, China

(Received 30 July 2020; revised manuscript received 23 September 2020; accepted manuscript online 15 October 2020)

Recently, the quantitative rescattering model (QRS) for nonsequential double ionization (NSDI) is modified by taking into account the potential change (PC) due to the presence of electric field at the time of recollision. Using the improved QRS model, we simulate the longitudinal momentum distributions of doubly charged ions He^{2+} by projecting the correlated two-electron momentum distributions for NSDI of He onto the main diagonal. The obtained results are compared directly with the experimental data at different intensities. It is found that when the PC is considered, the width of momentum distributions reduces and the agreement between theory and experiment is improved.

Keywords: nonsequential double ionization, quantitative rescattering model, potential change, momentum distribution of doubly charged ion

PACS: 34.50.Rk, 34.80.Dp, 32.80.Fb, 32.80.Rm **DOI:** 10.1088/1674-1056/abc151

1. Introduction

It has been widely accepted that the main mechanisms for non-sequential double ionization (NSDI) are the laser-induced recollision direct ionization (RDI) and the recollision excitation with subsequent ionization (RESI),[1] which can be qualitatively interpreted by the classical three-step rescattering model.[2] In the scenario of three-step model, an electron that was first released by tunneling through the barrier of combined atomic and field potential could then be driven back to the parent ion. Then the laser-induced returning electron may collide with the parent ion, leading to a secondary electron being ionized through RDI or RESI. This implies that NSDI takes place only when the kinetic energy of returning electron is sufficiently high to ionize an electron of the residual ion or to promote this electron to an excited state. According to the classical rescattering model, the maximum kinetic energy that a returning electron can accumulate in the field is $3.17U_{\rm p}$, where $U_{\rm p}$ is the ponderomotive energy that is proportional to the laser intensity. This indicates that a "threshold intensity" (the minimum intensity) for NSDI is required. However, NSDI processes have been observed to occur at intensity below the expected threshold intensity in the experimental measurements for both the total yields of doubly charged ions[3] and the correlated two-electron momentum distributions (CMDs)[4] as well.

It was argued[5] that the confliction of the recollision model with experimental observations arises from the assumption that scattering can be treated as if it takes place in a free atom. In a free atom or ion, the total energy of a continuum electron must be positive. Therefore, an incoming electron must possess a kinetic energy larger than the threshold energy for excitation to promote the ground-state electron to an excited state and remain a continuum electron. Nevertheless, this is not necessarily the case when the collision takes place in an electric field. Since the combined electric and atomic potentials form a barrier below zero, the incoming electron can escape from the atom or ion even with negative energy provided that its energy is higher than the potential barrier after the collision. As a result, even when the returning electron has an energy less than the energy difference between the ground state and the excited state, electron impact excitation of the parent ion can still take place in the laser-induced recollision process, since the returning electron can donate more energy to the ionic electron compared to the laser-free collisions. This is somehow equivalent to lowering of threshold, although the energy level of an excited state is not lowered. The lowering of threshold due to the presence of electric field is referred to as potential change (PC) in this paper.

The evidence of PC in NSDI was first provided by van der Hart and Burnett.[5] Using a recollision model, they performed the calculations on the ratio between double and single ionization for He atoms subjected to intense laser pulses. It was shown that by taking the laser field at the recollision into account, the recollision model used in Ref. [5] successfully reproduced the ratio between double and single ionization below threshold intensity.

The methodology proposed by van der Hart and Burnett

*Project supported by the National Natural Science Foundation of China (Grant No. 11274219), the Science and Technology Planning Project of Guangdong Province of China (Grant No. 180917124960522), and the Program for Promotion of Science at Universities in Guangdong Province of China (Grant No. 2018KTSCX062).

†Corresponding author. E-mail: jcc@ustc.edu.cn
‡Corresponding author. E-mail: chenzj@stu.edu.cn

© 2021 Chinese Physical Society and IOP Publishing Ltd

was recently adopted by Chen and collaborators in the quantitative rescattering (QRS) model.[6] With the PC considered, the QRS model was modified and employed to evaluate the yields of doubly charged ions due to NSDI of He and Ne by intense laser pulses at wavelengths of 800, 780, 400 and 390 nm, and the obtained results were found to be in good agreement with the experimental measurements over the entire intensity range including the intensities below threshold.[6–8] Very recently, using the modified QRS model, Chen *et al.*[9,10] simulated the CMD for NSDI of He. It was found that the CMD reproduced by the modified QRS model was in better agreement with the experimental measurements[11] than that predicted by the original QRS model, which confirms again the validity of the modifications made in the QRS model.

While the early measurements of the total yield of doubly charged ions as a function of the laser intensity[12] settled the controversial debate on the mechanisms responsible for NSDI, the measured momentum distributions of doubly charged ions[13] provide more insight into the ionization mechanism and hence offer more stringent test of the theoretical models. In this paper, we apply the QRS model to simulate the longitudinal momentum distributions of doubly charged ions for NSDI of He in 795 nm laser pulses. We make direct quantitative comparisons of our model results with the experimental measurements of de Jesus *et al.*[14] It turns out that with the PC taken into account, the agreement between theory and experiment is greatly improved, which provides, for the first time, the direct evidence of PC in NSDI above threshold intensity.

Unless indicated otherwise, atomic units (a.u.) are used throughout this paper.

2. Theoretical method

In this paper, we consider PC in the QRS model and investigate the effect of PC on the process of NSDI.

2.1. Potential change in NSDI

Suppose that we have an ion with effective charge Z in an electric field $F(t) = F_0\cos(\omega t)$, the combined electric field and Coulomb potentials along the polarization axis z of the laser field is given by

$$V(z) = F(t)z - \frac{Z}{|z|}. \tag{1}$$

As displayed in Fig. 1, a barrier appears when the electric field is added to the Coulomb potential. The maximum of the barrier in the combined Coulomb and electric field potentials is

$$V_{\rm b} = -2\sqrt{Z|F|}. \tag{2}$$

For electron impact excitation and ionization of a singly charged ion, $Z = 1$ and 2, respectively. Thus, for laser-induced electron impact excitation and electron impact ionization, the Coulomb potential is lowered by $|V_{\rm b}|$. This indicates that, in principle, the laser-induced returning electron with energy $E_{\rm r}$ has sufficient energy to promote a secondary electron from the ground state to an excited state when

$$E_{\rm r} > I_{\rm p}^{\rm exc} - \Delta E_{\rm exc}, \tag{3}$$

where $I_{\rm p}^{\rm exc}$ is the threshold energy for excitation and $\Delta E_{\rm exc} = -V_{\rm b}(Z = 1)$. For electron impact ionization, the minimum energy with which the secondary electron can escape is also lowered in the presence of an electric field. Therefore, in the case of double ionization, another term, corresponding to the barrier height, should be added. As a result, to eject a secondary electron, the kinetic energy of the returning electron should satisfy the condition[5]

$$E_{\rm r} > I_{\rm p}^{\rm e2e} - \Delta E_{\rm e2e}, \tag{4}$$

where $I_{\rm p}^{\rm e2e}$ is the threshold energy for ionization and $\Delta E_{\rm e2e} = -2V_{\rm b}(Z = 2)$.

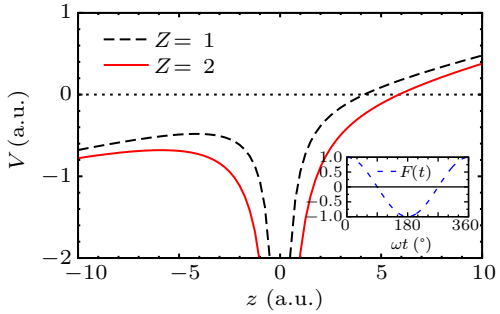


Fig. 1. Combined electric field potential $F(t) = F_0\cos(\omega t)$ and Coulomb potential with $Z = 1$ and $Z = 2$ along the polarization axis z of the laser field at an intensity of 10×10^{14} W/cm^2. The phase of the electric field is chosen to be $\omega t = 290°$. The inset shows the normalized monochromatic laser field.

Although the barrier height can be easily determined, it is far from straightforward to take the PC into account in the QRS model since recollision takes place at different times and the corresponding barrier height of the combined atomic and electric fields varies with the angle to the polarization axis. For simplicity, we choose an "average" returning time of $t = 290°/\omega$ in our calculations.[9] Unfortunately, even with this average returning time, it is still a formidable task to perform actual numerical calculations. Alternatively, we follow the prescription suggested by van der Hart and Burnett.[5] To account for the lowering of threshold, we adjust the collision energy so that the laser-free incoming electron energy $E_{\rm i}$ corresponds to the laser-induced returning electron energy

$$E_{\rm r} = E_{\rm i} - \Delta E_j, \tag{5}$$

where j stands for exc or e2e.

2.2. The QRS model for NSDI

We aim to evaluate the longitudinal momentum distributions of doubly charged ions for NSDI of He and compare the simulated results with the corresponding experimental findings.[14] The momentum distributions of doubly charged ions are obtained by projecting the CMD for NSDI onto the main diagonal. Since the details of the numerical procedures for simulations of the CMD for NSDI of helium atoms based on the QRS model have been presented in Refs. [8,9,15], here we only give a brief overview.

The main philosophy of the QRS model for laser-induced rescattering processes is that the momentum distributions for photoelectrons can be expressed as a product of the returning-electron wave packet (RWP) and the field-free scattering cross sections. Therefore, to simulate the CMD for NSDI of He, we first need to prepare the RWP, the triple-differential cross sections (TDCSs) for electron impact ionization and the differential cross sections (DCSs) for electron impact excitation of He^+. The RWP is evaluated based on the improved strong-field approximation for high-order above-threshold ionization.[16] For the laser-induced recollision processes of He^+ considered here, only the cross sections for the singlet spin channel should be used, since the two electrons involved in the process start in the singlet ground state of He, and their singlet coupling is preserved.[17] The singlet TDCS for laser-free (e, 2e) of He^+ are calculated using the BBK model,[18] in which the Coulomb interaction between the two outgoing electrons is accounted for. The singlet DCSs for laser-free electron impact excitation of He^+ are evaluated using the state-of-the-art multi-electron *B*-spline *R*-matrix close-coupling theory[19] for incident energies below 100 eV and the distorted-wave Born approximation[20] for higher energies. In this paper, only the DCSs for excitation to the excited states of $n = 2$ and $n = 3$ are calculated, since the excitation to higher states can safely be neglected based on the n^{-3} scaling law.

With all these ingredients well prepared, we are now ready to simulate the CMD for NSDI of He. In the QRS model, the CMD for RDI and RESI are simulated separately.

According to the QRS model, the CMD for RDI in a laser pulse at an intensity I for the momentum components $p_1^{\parallel}$ and $p_2^{\parallel}$ of the two outgoing electrons along the laser polarization direction can be expressed as

$$D_{\rm I}^{\rm RDI}(p_1^{\parallel}, p_2^{\parallel}) = \int_{I_{\rm p}^{\rm e2e}}^{\infty} {\rm d}E_{\rm i}\, D_{E_{\rm i}}^{\rm e2e}(p_1^{\parallel}, p_2^{\parallel})\, W_{\rm I}(E_{\rm i} - \Delta E_{\rm e2e}). \quad (6)$$

Here $D_{E_{\rm i}}^{\rm e2e}(p_1^{\parallel}, p_2^{\parallel})$ is the CMD for the laser-induced recollision $(e, 2e)$ process at incident energy $E_{\rm i}$ obtained by projecting the TDCS for laser-free (e, 2e) of He^+ onto the polarization direction and shifting the parallel momenta of the two outgoing electrons by $-A_{\rm r}$,[9] where $A_{\rm r}$ is the instantaneous vector potential at the time of recollision. In Eq. (6), the integral over $E_{\rm i}$ is performed to account for contributions from collisions at all incident energies weighted by the RWP, $W_{\rm I}(E_{\rm r})$, which represents the probability of the returning electron with energy $E_{\rm r}$.[16]

Similarly, the CMD for RESI is given by

$$D_{\rm I}^{\rm RESI}(p_1^{\parallel}, p_2^{\parallel}) = \int_{I_{\rm p}^{\rm exc}}^{\infty} {\rm d}E_{\rm i}\, D_{E_{\rm i}}^{\rm exc}(p_1^{\parallel}) \times D_{\rm I}^{\rm tun}(p_2^{\parallel})\, W_{\rm I}(E_{\rm i} - \Delta E_{\rm exc}), \quad (7)$$

where $D_{E_{\rm i}}^{\rm exc}(p_1^{\parallel})$ is the parallel momentum distribution for the returning electron with kinetic energy $E_{\rm i}$ after recollision that is obtained by projecting the DCS for electron impact excitation of the parent ion onto the polarization direction to which the parallel momentum of the projectile electron is shifted by $-A_{\rm r}$, and $D_{\rm I}^{\rm tun}(p_2^{\parallel})$ represents the momentum distribution of the electron tunneling-ionized from an excited state of the parent ion.

The parallel momentum distributions $D_{\rm I}^{\rm tun}(p_2^{\parallel})$ for tunneling ionization of electrons in the excited states are calculated by integrating the two-dimensional (2D) momentum distributions for single ionization over the momentum component perpendicular to the laser polarization. In the present study, the 2D momentum distributions for single ionization of He^+ are evaluated by solving the time-dependent Schrödinger equation[21] directly for laser intensities below 4.5×10^{14} W/cm^2. To save computational time, the strong field approximation (SFA)[22] is employed for higher intensities. The validity of SFA for intensities higher than 4.5×10^{14} W/cm^2 has been verified in Ref. [23].

The magnitude of vector potential $A_{\rm r}$ at the instant of recollision is determined by the returning electron energy,

$$|A_{\rm r}| = \sqrt{2E_{\rm r}}/1.26, \quad (8)$$

where $E_{\rm r}$ is given by Eq. (5).

3. Results and discussion

In this study, we focus on the parallel momentum distributions of the doubly charged ions for NSDI of He in 795 nm laser pulses at intensities of 6.0, 7.0, 10.0, and 12.5×10^{14} W/cm^2 measured by de Jesus *et al.*[14] Very recently, we investigated the intensity dependence in NSDI of He by strong laser pulses at 800 nm,[23] which is very close to the wavelength considered in the present work. In Ref. [23], the CMD for NSDI of He at intensities in the range from 2×10^{14} W/cm^2 to 15×10^{14} W/cm^2 have been simulated without taking into account PC, and the ingredients involved in the CMD, including the scattering cross sections for laser-free electron impact excitation and electron impact ionization, the parallel momentum distributions for the projectile electron after recollision and the tunneling-ionized electron have been presented. Here,

we therefore only show the parallel momentum distributions for the two correlated electrons and the doubly charged ions.

In Fig. 2, we plot the simulated CMD and the corresponding parallel momentum distributions of the doubly charged ion for RESI and RDI in NSDI of He by 795 nm laser pulse at an intensity of 10×10^{14} W/cm^2. First of all, it is obvious that PC plays an important role in producing the CMD for both RESI and RDI. By comparing Figs. 2(c) and 2(d) with Figs. 2(a) and 2(b), one can see that, with the PC effect taken into account, the CMDs for both RESI and RDI shrink such that the density in the CMD at smaller momenta increases. This is due to the fact that, according to Eqs. (5) and (8), the outgoing electrons in the recollision processes at a given incident energy are supposed to possess smaller drift momenta when the lowering of potential barrier is considered. As a result, as demonstrated in Figs. 2(e) and 2(f), in the parallel momentum distributions of He^{2+}, more probabilities for RESI at smaller momenta are generated and the 'valley' predicted by the original QRS model is almost filled. At the same time, the double peak in the distributions of RDI moves towards the center.

From Fig. 2, one can also see that, with the PC accounted for, the total yields for both RESI and RDI increase. Nevertheless, the relative increase for RDI is more pronounced than that for RESI since the PC for RDI is much larger than that for RESI. Take the peak intensity of 10×10^{14} W/cm^2 as an example, the maximum adjustments of the collision energy for the returning electron are 37 eV for RDI and 13 eV for RESI.

By adding the CMD for RESI to that for RDI, we obtain the entire CMD for NSDI. The CMD for NSDI of He, including both RESI and RDI, by 795 nm laser pulses at intensities of 6.0, 7.0, 10.0, and 12.5×10^{14} W/cm^2 are displayed in Fig. 3.

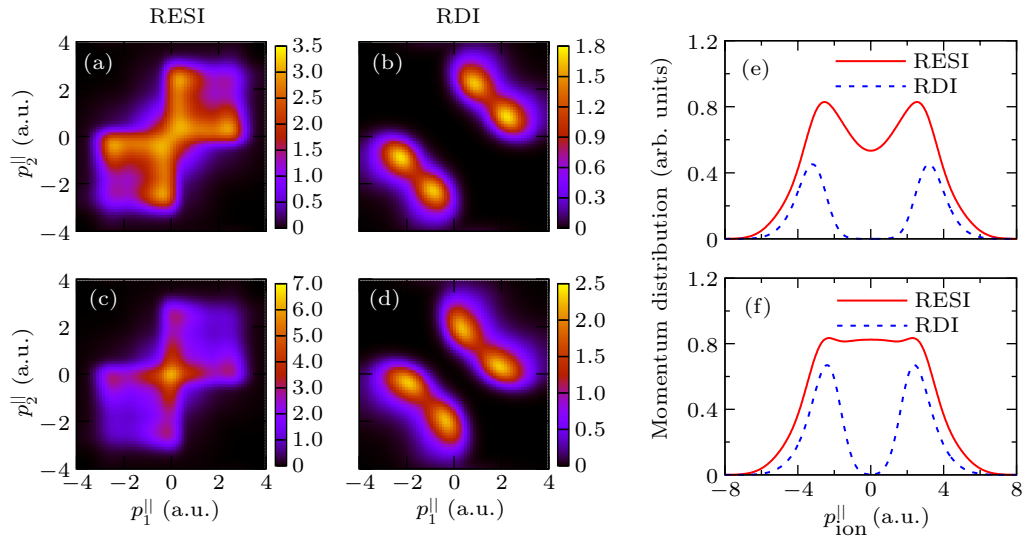


Fig. 2. Correlated two-electron momentum distributions for RESI and RDI in NSDI of He by a 795 nm laser pulse at an intensity of 10×10^{14} W/cm^2 [(a)–(d)] and the corresponding parallel momentum distributions of the doubly charged ion [(e), (f)]. The results without and with the potential change accounted for are shown in the first and the second rows, respectively.

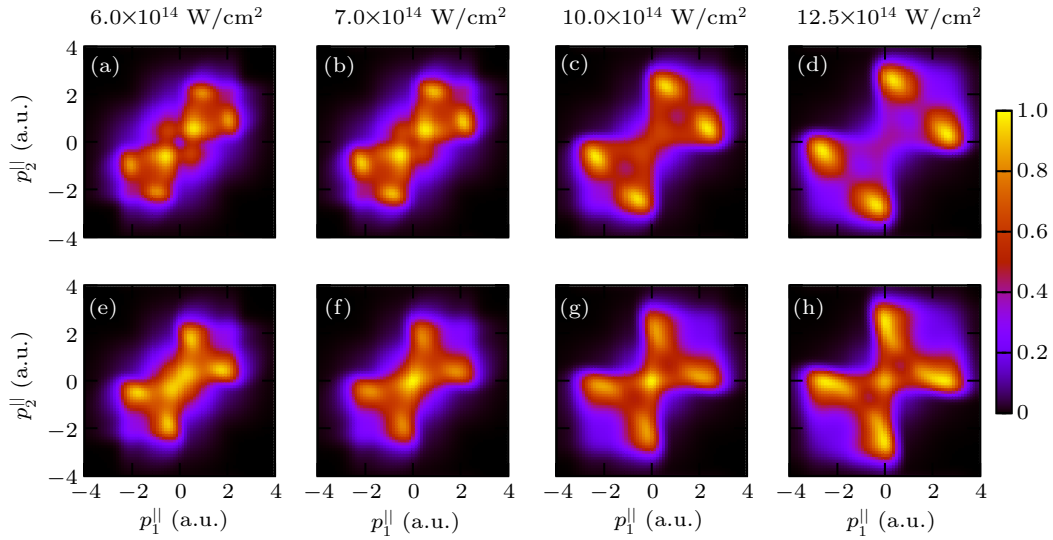


Fig. 3. Normalized correlated two-electron momentum distributions for NSDI of He by 795 nm laser pulses at intensities of 6.0, 7.0, 10.0, and 12.5×10^{14} W/cm^2. The results without and with the potential change accounted for are shown in the first and the second rows, respectively.

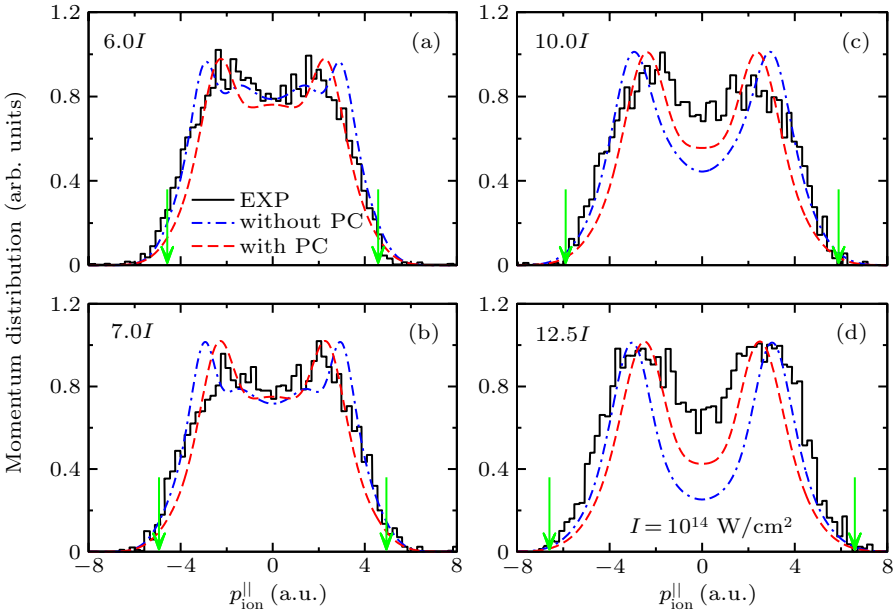


Fig. 4. Parallel momentum distributions of doubly charged ions for NSDI of He by 795 nm laser pulses at peak intensities of (a) 6.0, (b) 7.0, (c) 10.0, and (d) 12.5×10^{14} W/cm^2. The black solid line represents the experimental data taken from de Jesus *et al.*,[14] the blue chain and red broken curves are the simulated results without and with the potential change accounted for. The arrows indicate the upper limits for the kinematically favored ion momenta of $\pm 4\sqrt{U_p}$.

As is expected, the region of the CMD spreads as the intensity increases and, at a given intensity, the CMD is squeezed when the PC is considered. Furthermore, it should be noted that the maximum energy of the returning electron is proportional to the laser intensity. At 12.5×10^{14} W/cm^2, which is the highest intensity considered here, the maximum energy of the returning electron is about 235 eV. As demonstrated in Ref. [23], close to threshold, the total cross section for ionization increases rapidly until it reaches a maximum below 120 eV, and then decreases very slowly with increasing impact energy. On the other hand, the total cross section for excitation decreases steadily beyond a narrow maximum within about 15 eV above the threshold energy. Around 150 eV, the two cross sections become comparable. Therefore, the relative contribution from RDI is enhanced with the increase of intensity. This explains why the momentum distributions in the outer part in the first and third quadrants become denser at higher intensities.

The parallel momentum distributions of doubly charged ions obtained by projecting the CMD for NSDI onto the main diagonal $p_1^{\parallel} = p_2^{\parallel}$ are shown in Fig. 4, where the corresponding experimental measurements[14] are also displayed for comparison. For all the situations considered here, a double-hump structure was observed in experiments. As the intensity increases, the momentum distributions become broader and the double-hump is more pronounced. While the characteristic double-hump structure and the general pattern of the ion momentum distributions have been successfully predicted by the QRS model, the agreement with experimental measurements is greatly improved when the PC is taken into account. It can be seen that the width between the two peaks reproduced by the modified QRS model exactly matches the experimental findings, whereas the original QRS model without considering the PC effect generated a wider double-hump not consistent with experiment. The main discrepancies between theory and experiment exist at high intensities of 10.0 and 12.5×10^{14} W/cm^2. In these situations, compared to the experimental measurements, a deeper minimum at zero momentum in the double-hump is predicted even with the PC accounted for. This may indicate that the contributions from RDI are overestimated. Since the cross sections for both ionization and excitation were calculated based on the full quantum collision theory, the possible reason leading to the overestimation of RDI could be the approximation made in the evaluation of potential change. Instead of choosing an average returning time in the calculations, the potential change at each returning time should be considered individually. Further work will be performed to remedy this deficiency.

Finally, we emphasize that in all the simulated results presented in this paper, the focal volume averaging has been considered.

4. Conclusions

Using the QRS model with and without taking into account the potential change due to the presence of electric field at the instant of recollision, we have simulated the parallel momentum distributions of doubly charged ions for NSDI of helium by 795 nm laser pulses at intensities of 6.0, 7.0, 10.0 and 12.5×10^{14} W/cm^2. The model results are compared directly with the corresponding experimental measurements. It is found that when the potential change is considered, the width between the two peaks becomes narrower

and the minimum at zero momentum increases. Both of these changes in the simulated ion momentum distributions improve the agreement of the model results with experimental findings. The present investigations provide clear evidence of potential change in NSDI at intensities above the threshold.

We comment that, besides the total yields of the doubly charged ions measured at intensities below the threshold intensity,[5–7] the potential change effect has also been observed in the experimental measurements of CMD at intensities above the recollision threshold.[10] Although the CMD provides more detailed information than the longitudinal momentum distribution of doubly charged ions, direct quantitative comparisons between theory and experiment are hampered due to the two-dimensional data of CMD. In this sense, we believe that to show the direct evidence of potential change effect in NSDI above-threshold intensity, the one-dimensional longitudinal momentum distribution is the best candidate.

References

[1] Feuerstein B, Moshammer R, Fischer D, Dorn A, Schröter C D, Deipenwisch J, Crespo Lopez-Urrutia J R, Höhr C, Neumayer P, Ullrich J, Rottke H, Trump C, Wittmann M, Korn G and Sandner W 2001 *Phys. Rev. Lett.* **87** 043003

[2] Corkum P B 1993 *Phys. Rev. Lett.* **71** 1994

[3] Sheehy B, Lafon R, Widmer M, Walker B, DiMauro L F, Agostini P A and Kulander K C 1998 *Phys. Rev. A* **58** 3942

[4] Liu Y, Ye D, Liu J, Rudenko A, Tschuch S, Dürr M, Siege M, Morgner U, Gong Q, Moshammer R and Ullrich J 2010 *Phys. Rev. Lett.* **104** 173002

[5] van der Hart H W and Burnett K 2000 *Phys. Rev. A* **62** 013407

[6] Chen Z, Zheng Y, Yang W, Song X, Xu J, DiMauro L F, Zatsarinny O, Bartschat K, Morishita T, Zhao S F and Lin C D 2015 *Phys. Rev. A* **92** 063427

[7] Chen Z, Li X, Zatsarinny O, Bartschat K and Lin C D 2018 *Phys. Rev. A* **97** 013425

[8] Chen Z, Zhang L, Wang Y, Zatsarinny O, Bartschat K, Morishita T and Lin C D 2019 *Phys. Rev. A* **99** 043408

[9] Chen Z, Wang Y, Zhang L and Jia X 2019 *Phys. Rev. A* **99** 033401

[10] Chen Z, Wang Y, Morishita T, Hao X, Chen J, Zatsarinny O and Bartschat K 2019 *Phys. Rev. A* **100** 023405

[11] Staudte A, Ruiz C, Schöffler M, Schössler S, Zeidler D, Weber Th, Meckel M, Villeneuve D M, Corkum P B, Becker A and Dörner R 2007 *Phys. Rev. Lett.* **99** 263002

[12] Walker B, Sheehy B, DiMauro L F, Agostini P, Schafer K J and Kulander K C 1994 *Phys. Rev. Lett.* **73** 1227

[13] Weber Th, Weckenbrock M, Staudte A, Spielberger L, Jagutzki O, Mergel V, Afaneh F, Urbasch G, Vollmer M, Giessen H and Dörner R 2000 *Phys. Rev. Lett.* **84** 443

[14] de Jesus V L B, Feuerstein B, Zrost K, Fischer D, Rudenko A, Afaneh F, Schröter C D, Moshammer R and Ullrich J 2004 *J. Phys. B: Atom. Mol. Opt. Phys.* **37** L161

[15] Chen Z, Liu F and Wen H 2019 *Chin. Phys. B* **28** 123401

[16] Chen Z, Le A T, Morishita T and Lin C D 2009 *Phys. Rev. A* **79** 033409

[17] Yudin G L and Ivanov M Y 2001 *Phys. Rev. A* **64** 035401

[18] Brauner M, Briggs J S and Klar H 1989 *J. Phys. B* **22** 2265

[19] Zatsarinny O and Bartschat K 2013 *J. Phys. B* **46** 112001

[20] Liang Y, Chen Z, Madison D H and Lin C D 2011 *J. Phys. B* **44** 085201

[21] Morishita T, Chen Z, Watanabe S and Lin C D 2007 *Phys. Rev. A* **75** 023407

[22] Chen Z, Morishita T, Le A T and Lin C D 2007 *Phys. Rev. A* **76** 043402

[23] Chen Z, Wen H, Liu F, Morishita T, Zatsarinny O and Bartschat K 2020 *Opt. Express* **28** 6490